Pergamon

0094-5765(95)00006-2

Acta Astronautica Vol. 35, No. 8, pp. 489–500, 1995

0094-5765/95 $9.50 + 0.00

OPTIMAL MASS FOR AEROBRAKING TETHERS†

J. M. LONGUSKI, J. PUIG-SUARI, P. TSIOTRAS and S. TRAGESSER
School of Aeronautics and Astronautics, Purdue University, West Lafayette, IN 47907-1282, U.S.A.

(Received 12 August 1994)

Abstract—Earlier work has demonstrated the feasibility of using aerobraking tethers for the exploration of the solar system. In fact, compared to chemical propulsion, the tether mass is usually much less than the required propellant mass. The basic concept involves an orbiter and a probe connected by a thin tether. The probe is deployed into the atmosphere of a planet where aerodynamic drag decelerates it. The tension on the tether provides the braking effect on the orbiter, thus eliminating the need for a propulsive maneuver. During the maneuver the orbiter travels outside the atmosphere, and does not require heat shielding. In the previous work a suboptimal solution was found where the system maintained a near vertical orientation during the fly through. In this paper we consider the minimum tether mass required for specified aerocapture conditions. As an intermediate step, we find the trajectory which provides the minimum tension on the tether. The fact that the orbiter must remain outside the atmosphere is introduced as an altitude constraint. The results are significant for future solar system exploration.

1. INTRODUCTION

In the history of the exploration of the solar system, some of the most successful and most ambitious missions have involved dual vehicle spacecraft. In such a mission (the Viking program being the best known) one vehicle (a probe or lander) is delivered to the planet's surface or atmosphere, while the second one (the orbiter) remains in orbit around the planet. The Galileo spacecraft, currently on its way to Jupiter, is representative of several missions being proposed in this category. When the spacecraft arrives at the target planet, the orbiter performs a propulsive maneuver to achieve capture, while the probe relies on an aerobraking maneuver to decelerate.

The aerobraking tether shown in Fig. 1 eliminates the need for the orbiter propulsive maneuver. The spacecraft consists of an orbiter and a probe that are connected by a thin tether. When the vehicle arrives at the planet, the probe flies into the atmosphere, as before, while the orbiter is decelerated by tether tension, thus eliminating the need for propellant. Note that the orbiter remains outside the atmosphere during the maneuver and does not require additional aerodynamic shielding. After capture has occurred, the tether may be severed, allowing the probe to land on the planet, or the system may remain together and additional aerobraking maneuvers can be performed to finalize the orbit.

The concept of using tethers for aeroassisted maneuvers has appeared in the literature as early as 1986, being mentioned by Carroll [1] and Purvis and Penzo [2]. The idea was previously proposed at the Jet Propulsion Laboratory in 1984 by Sirlin *et al.* [3]. Despite the early introduction of the aerobraking tether idea and the great interest that tethers in space have received in recent years, work on tethers in an atmosphere has been very limited. Lorenzini *et al.* [4] analyzed the behavior of a tethered system in the Martian atmosphere, but the spacecraft was maintained in circular orbit using thrusters. More recently, Warnock and Cochran [5] studied the orbital lifetime of tethered satellites. This is a very complete analysis of orbit decay but no attempt was made to use the drag for maneuvering.

Analysis by Puig-Suari and Longuski [6] involved modeling the tether as a rigid rod with the conjecture that, if aerobraking is feasible with such a simple model, then a more involved study would be warranted. This conjecture is supported by the early work of Lorenzini *et al.* [4], which demonstrates that a flexible tether, subjected to aerodynamic loads, remains relatively straight, at least in a circular orbit. Even though the rigid rod model does not include flexible effects, it retains the essential behavior of the system by taking into account distributed gravitational and aerodynamic forces. Using this model, Puig-Suari and Longuski demonstrate the physical feasibility of aerobraking with a tether in [6] and [7].

In [8], Puig-Suari and Longuski deal with the difficult task of finding targeting conditions. Simple analytical models are developed to facilitate the determination of the initial conditions required for aerocapture. First, an analytical approximation for

†Paper IAF-93-A.2.13 presented at the *44th International Astronautical Congress*, Graz, Austria, 16–22 October 1993.

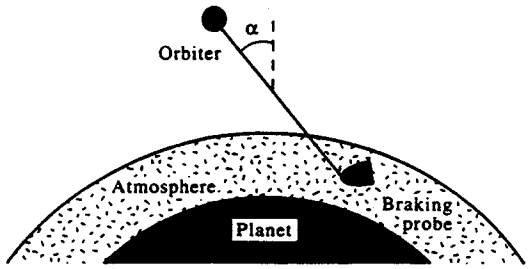

Fig. 1. Aerobraking tether.

the change in velocity during the atmospheric portion of the trajectory is found in terms of error functions. Next, perturbation techniques are used to determine approximate equations for the motion of the system outside the atmosphere (i.e. with no aerodynamic effects). These two approximate models provide a way to determine a good first guess for initial conditions. The precise initial conditions are found iteratively by performing numerical analysis with the (much more complicated) complete rigid rod model. This makes it possible to define and simulate the behavior of many types of tether aerocapture maneuvers.

Longuski *et al.* [9] compare the performance of the tether system with that of the traditional propulsive maneuver in missions to all the atmosphere-bearing planets in the solar system. The relative performance of the two systems is determined by comparing the mass of the tether and the mass of the propellant required to capture the orbiter. Despite the fact that no attempt is made to determine the minimum tether mass required for the maneuvers, the results show a clear mass advantage in the tethered system.

The results obtained with the rigid rod are very encouraging, but the flexibility of a real tether may have detrimental effects on the performance of the system. In [10] and [11] flexible tether models are developed to permit the analysis of more realistic tethered systems. The results obtained with the flexible models indicate that the basic behavior of the tethered system is very similar to that observed with the rigid rod model. This validates the earlier conjecture that the rigid rod model might serve as a reasonable tool for the preliminary assessment of tether aerobraking problems. In fact (when the proper care is exercised) the rigid rod model is very faithful to the actual behavior so that flexible analysis is only necessary in the final stages of the design process.

In this paper optimization techniques are used to determine the aerobraking maneuver which minimizes the tether mass. The optimum maneuver may be used to increase the already significant mass advantage of the tether aerobraking system over the traditional propulsive maneuvers.

2. AEROBRAKING TETHER DESIGN CONCEPTS AND RESULTS

In [9] aerobraking tether design concepts are developed for the exploration of the solar system. The model used in the analysis assumes a rigid tether, planar motion and an exponential atmosphere. The study includes missions to Venus, Mars, Jupiter, Saturn, Uranus, Neptune, Titan and a Mars–Earth return mission. In this preliminary study, certain specifications are made which ultimately lead to unique designs for braking into a capture orbit about these planets. These specifications include the following.

(1) The fly-through maneuver (Fig. 2) is designed so that the inertial spin rate during atmospheric entry, $\mathbf{\Omega}_{in}$, is equal and opposite to the spin rate during exit, $\mathbf{\Omega}_{out}$

$$\mathbf{\Omega}_{out} = -\mathbf{\Omega}_{in} \tag{1}$$

This requirement is called spin matching.

(2) The tether length is specified so that the location of the center of pressure with respect to the probe, l_{ps}, coincides with that of the center of percussion, l_{pc}. This requirement is called center matching:

$$l_{ps} = l_{pc} \tag{2}$$

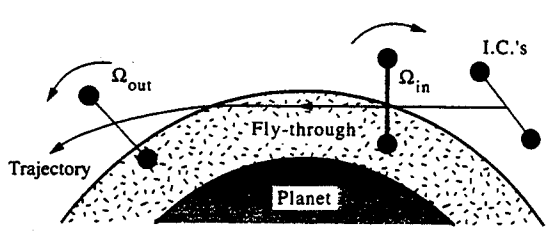

Fig. 2. Aerobraking maneuver.

(3) The ballistic coefficient of the probe is equal to the ballistic coefficient of the tether:

$$\eta/(C_{Dt}d) = m_p/(C_{Dp}S_p) \quad (3)$$

where η is the tether linear density, which depends on the tether mass and its dimensions, C_{Dt} and C_{Dp} are the drag coefficients of the tether and the probe, respectively, d is the diameter of tether and S_p is the frontal area of the probe. In [9] the values assumed for C_{Dt} and C_{Dp} are 2 and 1, respectively. This requirement is called aeromatching.

(4) The mass of the orbiter, m_o, and the mass of the probe, m_p, are both assumed to be equal to 1000 kg:

$$m_o = m_p = 1000 \text{ kg} \quad (4)$$

(5) The tether is assumed to be Hercules AS4 graphite [12] with a tensile strength, σ_u, and a density, ρ_t:

$$\sigma_u = 3.6 \text{ GN/m}^2$$

$$\rho_t = 1800 \text{ kg/m}^3 \quad (5)$$

(6) The planets are assumed to be in circular, co-planar orbits. Arrival conditions are calculated by assuming an interplanetary Hohmann transfer. The spacecraft is then captured into a near-parabolic orbit about the target planet so that:

$$e = 0.9999 \quad (6)$$

(where e is the eccentricity with respect to the planet).

From conditions (1)–(3), and assuming that the tether is nearly vertical at closest approach, it is shown in [9] that the mass of the tether is approximated by:

$$m_t = \frac{\rho_t m_o(m_o + m_p)}{4\sigma_u m_p}\Delta V^2 \quad (7)$$

where ΔV is the change in velocity required at the target planet in order to achieve capture.

In [9] a comparison is made between the mass of the tether [eqn (7)] and the propellant mass required (to slow down the orbiter) with a chemical rocket system, Δm:

$$\Delta m = m_o(e^{(\Delta V)/(I_{sp}g)} - 1) \quad (8)$$

where g is the acceleration due to gravity at the Earth's surface and I_{sp} is the specific impulse. The value for I_{sp} is assumed to be 300 s. The results of this comparison, presented in Table 1, are quite exciting because in every case the tether mass is smaller than the required propellant mass. The greatest absolute savings occur at Mars (144 kg) and the greatest percentage savings are found at Jupiter (81%). The design tension, computed by the simple formula [9]

$$T = \frac{m_o(m_o + m_p)}{4m_p l}\Delta V^2 \quad (9)$$

is a very good approximation for the actual tension observed in the simulation of the fly-through maneuver.

In every case, the design specifications (1)–(3) result in a tether length of approx. $1.8H$ (scale heights), so that the maximum atmospheric density at the probe is approx. 6 times ($e^{1.8}$ times) larger than that at the orbiter. The difference between the orbiter minimum height and the probe minimum height is nearly the full length of the tether, which reflects the fact that the tether is in a local vertical position, as desired, during the closest approach phase.

The specific characteristics of the Mars maneuver are shown in Figs 3–5. Figure 3 shows the radius of

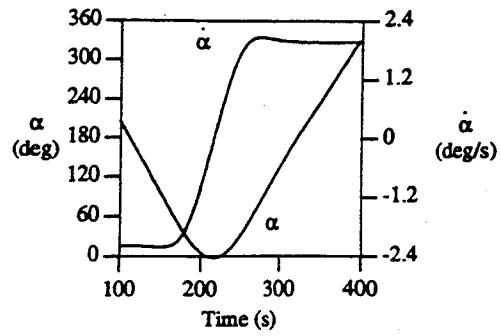

Fig. 4. Orientation angle, α, and $\dot{\alpha}$.

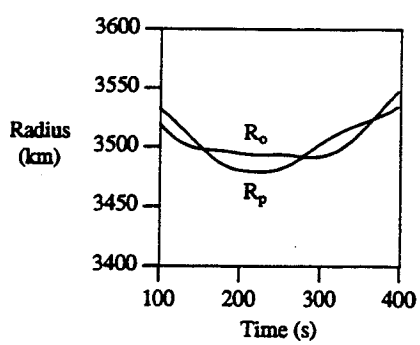

Fig. 3. Orbiter and probe trajectories.

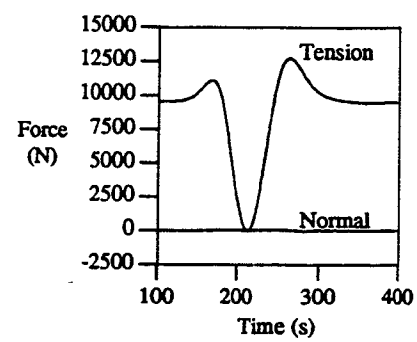

Fig. 5. Tension and normal forces on probe.

Table 1. Aerocapture results for solar system exploration (vertical dumbbell design)

Values	Venus	Earth	Mars	Jupiter	Saturn	Uranus	Neptune	Titan
ΔV (km/s)	0.35	0.39	0.67	0.27	0.41	0.50	0.34	1.31
Propellant mass (kg)	126	142	256	96	149	185	122	559
Tether mass† (kg)	31.0	38.0	112	18.0	42.0	63.0	29.0	426
Savings (%)	75%	73%	56%	81%	72%	66%	76%	24%
Savings (kg)	95.0	104	144	78.0	107	122	93.0	133
Length (km)	10.8	9.0	14.5	36.1	54.4	72.7	72.7	84.2
Diameter (mm)	1.42	1.73	2.34	0.600	0.740	0.780	0.530	1.89
Probe area (m^2)	999	818	605	2370	1910	1810	2670	747
Design tension (N)	5670	8450	15500	1010	1550	1720	795	10100
Actual tension (N)	5430	7850	12700	1050	1630	1860	899	9443
% of design	96%	93%	82%	104%	105%	108%	113%	93%
Orbiter ρ_{max} (kg/m^3)	5.02×10^{-8}	5.39×10^{-8}	2.18×10^{-7}	4.81×10^{-10}	1.73×10^{-9}	3.29×10^{-9}	1.31×10^{-9}	5.21×10^{-7}
Probe ρ_{max} (kg/m^3)	3.04×10^{-7}	3.27×10^{-7}	1.42×10^{-6}	2.92×10^{-9}	1.05×10^{-8}	2.04×10^{-8}	8.14×10^{-9}	2.28×10^{-6}
Orbiter h_{min} (km)	146	103	93	495	848	1496	1246	522
Probe h_{min} (km)	135	94	81	459	794	1423	1173	456
Atmosphere								
Scale height (km)	6	5	8	20	30	40	40	45
Ref. altitude (km)	6150	6458	3507	71592	60350	26145	24750	2738
Ref. density (kg/m^3)	1.0×10^{-4}	7.7×10^{-6}	5.5×10^{-8}	1.85×10^{-3}	2.8×10^{-2}	4.69×10^{-1}	5.76×10^{-1}	1.7×10^{-3}
Hohmann transfer								
Gravity constant (km^3/s^2)	3.25×10^5	3.99×10^5	4.28×10^4	1.27×10^8	3.79×10^7	5.80×10^6	6.85×10^6	9.0×10^3
Radius (km)	6.05×10^3	6.38×10^3	3.40×10^3	7.14×10^4	6.00×10^4	2.54×10^4	2.43×10^4	2.58×10^3
V_∞ (km/s)	2.71	2.97	2.65	5.64	5.44	4.66	4.05	4.01
Approach e	1.14	1.14	1.57	1.02	1.05	1.10	1.06	6.50
Approach r_{per}	6190	6480	3490	71900	60800	26900	25500	3080

†Approximated from eqn (7).

the orbiter, R_o, and of the probe, R_p, with respect to the center of the planet. Note that the radius of Mars is 3398 km. During atmospheric fly through the minimum altitudes of the orbiter and the probe are 92.5 and 80.7 km, respectively. The difference between these values is nearly the length of the tether. Next, the orientation of the tether, α (with respect to the local vertical), and its spin rate, $\dot{\alpha}$, are shown in Fig. 4. The graph clearly shows that during fly through the tether remains at a near vertical orientation ($\alpha = 0$). The values of the normal and tension forces at the probe end of the tether are plotted in Fig. 5 (the forces on the orbiter are very similar). The graph shows that forces due to spin are equal before and after impact (due to the spin matching condition). Also, the normal force is close to zero, which was one of the goals of the design. Note that the tether designed for this maneuver has an ultimate strength of 15,500 N [from eqn (9)] which is higher than the maximum value of tension observed in the simulation. Also note that the actual tension due to spin is, in this case, overestimated by eqn (9).

The promising results obtained in [9] and summarized in Table 1 for the rigid rod model demand that a deeper examination of the potential of aerobraking tethers be made. In the following analysis, we examine the question of optimal tether mass.

3. OPTIMAL TETHER MASS MANEUVERS

In the analysis performed in [9], the design process is structured to develop an aerobraking maneuver that requires a low tether mass (i.e. a low tether strength) in order to compete favorably with the propulsive systems. However, the starting point in the analysis assumes a dumbbell type maneuver, with the tether in a nearly vertical orientation at periapsis. In [8], a vast range of maneuvers seems possible between the extremes represented by the (vertical) dumbbell and (horizontal) drag chute maneuvers, and the possibility that some of these maneuvers may result in lower tether masses remains unexplored. One of the reasons to address the dumbbell case first is the ease with which the normal forces can be analyzed and the system designed to eliminate them. This requirement arises from the fact that the rigid rod model lacks the sophistication to incorporate the bending associated with normal forces. The development of the flexible models in [10] and [11] validates the rigid rod as an excellent design tool and also allows the analysis of a wider variety of tethered systems. At this point, a more systematic analysis of the possible tether aerobraking maneuvers is not only possible but also very desirable.

Before we proceed in the next section with the optimization problem, we should mention briefly that optimization problems, in general, can take many iterations to converge and can be very sensitive to computational round-off and/or truncation errors. This is especially true for most practical problems—like the one treated in the present paper—where no explicit formulae for the gradient or the Hessian of the cost function are available. One must resort to numerical calculation of these quantities using finite difference methods, thus introducing an additional error in the calculations. Most optimization algorithms therefore benefit from good starting guesses for the solution. A good starting guess, apart from the fact that it can accelerate the convergence of the algorithm, can lead to the global rather than to a local minimum. One therefore has to be very careful in choosing initial guesses. Experience, judgement and (sometimes) luck can be the difference between success (convergence) and failure (divergence). Therefore, very complex problems are best solved by an evolutionary approach, whereby a problem with a smaller number of independent variables is solved first. Solutions from lower order problems can then be used as starting points for more complex problems with more independent parameters.

With this philosophy in mind we first solve the minimum force problem for an aerobraking tether. In this formulation the length of the tether is kept fixed, and the optimization algorithm will provide the minimum force maneuver for the given tether. One can then redesign the tether (e.g. change its diameter) to withstand the required force by the minimum amount of mass. Therefore, the minimum force solution for a given length of the tether is dual to the problem of minimum mass for this tether length. The results of the minimum force problem can then be used, as mentioned earlier, as good initial guesses for the complete minimum mass problem, where the length of the tether is among the design parameters.

3.1. *Minimum force analysis*

We initiate the search for the optimal tether maneuver by determining the aerobraking maneuver that minimizes the forces on the tether. For a given design, this optimum maneuver can be analyzed as a constrained optimization problem and solved using non-linear programming techniques. Once the physical parameters for the system are specified, the tether aerobraking maneuver can be defined by three parameters: the initial conditions outside the atmosphere, α_0 and $\dot{\alpha}_0$, and the radius of periapsis for the hyperbolic orbit, r_{per}. Thus the optimization process involves the search for the optimum initial conditions in a three dimensional parameter space. For the analysis presented here, the total force on the tether is defined as the (magnitude of the) vector addition of the tension and normal forces. Note that, for a given set of initial conditions, determination of the maximum force requires the computation of the complete atmospheric fly-through maneuver. Therefore the maximum force is computed only *a posteriori*. Clearly, an analytic computation of the gradients of the cost (i.e. force) with respect to the design parameters is out of the question. In addition, some constraints must be placed on the problem in order

to assure that the resulting optimum trajectory provides an acceptable aerobraking maneuver. First, we provide the value of the final orbit eccentricity that must be achieved by the maneuver, e_c, and introduce it as an equality constraint. Next, the objective of keeping the orbiter higher than the probe is introduced as an inequality constraint on the difference in the minimum altitudes of the orbiter and the probe, Δh_c, during the maneuver. Finally, the presence of compressive forces on the tether is prevented with an additional inequality constraint. Mathematically the problem can be written as:

$$\text{minimize:} \quad F_{\max}(x)$$

$$x = [\alpha_0, \dot{\alpha}_0, r_{\text{per}}]^t \tag{10}$$

$$\text{subject to:} \quad e - e_c = 0 \tag{11}$$

$$\Delta h - \Delta h_c > 0 \tag{12}$$

$$T_{\min} > 0 \tag{13}$$

where e and Δh are the eccentricity and altitude difference achieved by the maneuver and $T_{\min}$ is the minimum tension on the tether.

A large variety of techniques exists to solve a problem of the form given above. In this paper optimization software based on the exterior penalty method [13,14] is applied to the tether problem. This method incorporates the active constraints in the objective function by performing successive unconstrained minimizations of the function:

$$F_k = F_{\max}(x) + r_k \sum_{j=1}^{3} G_j(x), \quad k = 1, 2, 3, \ldots$$

and increasing the value of the factor, r_k, after each iteration. Here $G_j(x)$ is some function of the constraints g_j ($j = 1, 2, 3$) and r_k is a positive constant known as the penalty parameter. For our analysis we choose

$$G_j(x) = \{\max[0, g_j(x)]\}^2$$

The unconstrained minimizations are performed using Powell's method with a golden section method for the one-dimensional minimizations [13,14]. In the optimization procedure, the rigid rod model is the only practical model due to the large number of iterations required. (Typically the force optimization process requires several hours of CPU time on a Sun Sparc 10 workstation using the rigid rod model.) The validity of the optimum maneuver can be determined by performing a flexible analysis after the optimization process, as in [15].

The optimization method is first applied to the Mars aerocapture design [9,15]. The parameters are taken directly from the results of that maneuver (see Table 1 where $e = 0.9999$ and $\Delta h = 12$ km). The resulting optimum maneuver (see Figs 6 and 7) is significantly different from the maneuver described in Figs 4 and 5. During the optimal fly through, the minimum orientation angle of the tether is greater than zero. This fly-through angle means that the tether is subjected to significant tension at all points in the trajectory, which reduces the tendency to bend (in a flexible tether). In addition to these favorable characteristics, the maneuver reduces the forces from over 12,000 N (Table 1) to 9000 N while achieving the same eccentricity. (Note in Fig. 7 the large reduction over Fig. 5 in the forces before and after impact due to the reduction in spin rate.) Small normal forces appear in the maneuver since the effective area of the tether is reduced by the fly-through orientation and this slightly offsets the aeromatching condition. Also note that the spin-matching condition emerges, in a natural way, as part of the optimum solution.

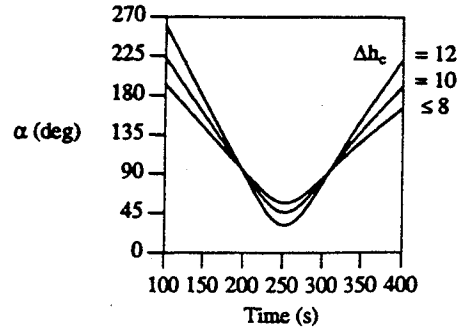

Fig. 6. Orientation angle (optimum force trajectories).

We observe that the altitude constraint is active in the previous maneuver ($\Delta h_c = 12$ km), and wish to investigate the effect of a reduction of the Δh_c requirement. When this is done the forces are further reduced as the Δh_c requirement is relaxed, until a value of 8 km is reached. Beyond this point, any further reductions in Δh_c have no effect on the maneuver (see Figs 6 and 7). Thus, the optimum maneuver for an unconstrained clearance maintains a clearance of 8 km. In this maneuver, the forces are reduced to the minimum value of about 7000 N, with a fly-through orientation of about 55° at closest approach.

The results of further investigation into the minimum force problem with unconstrained altitude are presented in Table 2 for the Mars tether with different

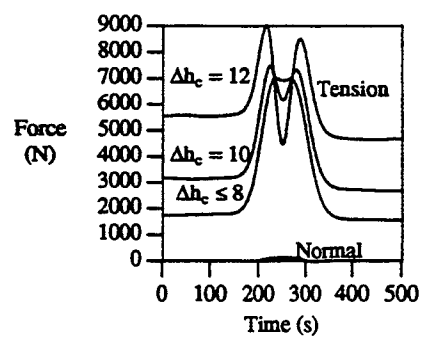

Fig. 7. Forces on the probe (optimum force trajectories).

Table 2. Mars minimum force results for unconstrained altitude†

e	ΔV (km/s)	α_{min} (degrees)	Δh	F_{max} (N)
0.50	1.33	64.0 (72.5)	3.82	14,400 (13,200)
0.75	0.983	62.2 (67.7)	5.65	10,700 (9720)
0.99	0.676	55.3 (60.2)	8.21	6990 (6620)
1.20	0.422	39.2 (48.4)	11.3	3990 (3970)
1.40	0.192	30.1 (28.0)	12.5	1260 (1370)
1.50	0.0819	−0.660 (17.1)	14.5	249 (356)

†Values in parentheses were predicted from eqn (47).

target eccentricities. In Fig. 8 we plot the maximum tether force, F_{max}, and the minimum orientation angle, α_{min}, against ΔV. We see that F_{max} increases nearly linearly with ΔV while α_{min} asymptotically approaches 90°, which is equivalent to a drag chute maneuver. For low ΔV, the α_{min} is nearly zero, approaching the vertical dumbbell maneuver. We will refer to this new type of maneuver (i.e. a maneuver having non-zero α_{min}) as an inclined maneuver.

3.2. Sliding pendulum model

During minimum force fly through we notice that near the time of closest approach, the tension force remains nearly constant, when the altitude is unconstrained. This is evident in the plateau that appears in Fig. 7 for $\Delta h_c \leqslant 8$. Another interesting feature that can be observed is that the orbiter altitude remains nearly constant during the atmospheric fly through, while the probe swings down into the atmosphere. This behavior is apparent in both the vertical dumbbell maneuver (Fig. 3) as well as in the optimal force and optimal mass solutions [15]. The pendulum motion of the probe suggests that the orbiter–probe–tether system can be modeled as a sliding pendulum, where the orbiter represents a sliding attachment point and the probe and tether represent the pendulum (see Fig. 9). In this motion the probe swings down to a minimum orientation angle, α_{min}, and is bounced back up and out of the atmosphere, while the orbiter maintains a nearly constant altitude. With this behavior in mind, we will attempt to construct a simple analytic model of the tension force in order to better understand the dynamics of the problem and to guide the numerical determination of the minimum force and minimum mass trajectories.

The ΔV obtained from the atmospheric fly through can be approximated by an impulse analysis for a particle [16,17]:

$$\Delta V = r_{per} V_{per} \sqrt{\frac{2\pi(1+e)}{\beta r_{per} e}} \frac{\rho_{per} C_D A}{2m} \tag{14}$$

(To find the impulsive ΔV for the entire tether see [8]. For a more sophisticated analysis of atmospheric fly through see Vinh *et al.* [18] and Vinh [19]). Equation (14) is given in terms of periapsis conditions, as indicated by the subscript "per", so that r_{per} is the radius at periapsis, V_{per} is the velocity at periapsis and ρ_{per} is the atmospheric density at periapsis. The drag coefficient, C_D, corresponds to a cross sectional area of A. The variable e is the approach eccentricity, relative to the planet or satellite. The term β is the inverse scale height ($\beta = 1/H$). (It is interesting to note that, according to Vinh [19], the product βr_{per} is nearly constant for variable r_{per} and β.)

Since the drag at periapsis is given by

$$D_{per} = \tfrac{1}{2}\rho_{per} C_D A V_{per}^2 \tag{15}$$

we can write, from eqn (14), that

$$\tfrac{1}{2}\rho_{per} C_D A = \frac{m\Delta V}{r_{per} V_{per}} \sqrt{\frac{\beta r_{per} e}{2\pi(1+e)}} \tag{16}$$

so that the drag can be rewritten as

$$D_{per} = m\Delta V \sqrt{\frac{\beta r_{per} e}{2\pi(1+e)}} \frac{V_{per}}{r_{per}} \tag{17}$$

Noting that the velocity at periapsis can be expressed in terms of the local circular speed, V_{lc}, we have

$$V_{per} = \sqrt{\frac{\mu}{r_{per}}(1+e)} = \sqrt{1+e}\, V_{lc} \tag{18}$$

and we obtain

$$D_{per} = m\Delta V \sqrt{\frac{\beta r_{per} e}{2\pi}} \frac{V_{lc}}{r_{per}} \tag{19}$$

The expressions for drag [eqn (19)] and ΔV [eqn (14)] imply that a characteristic fly-through time can be computed as

$$\Delta t = \frac{m\Delta V}{D_{per}} = \sqrt{\frac{2\pi}{\beta r_{per} e}} \frac{r_{per}}{V_{lc}} \tag{20}$$

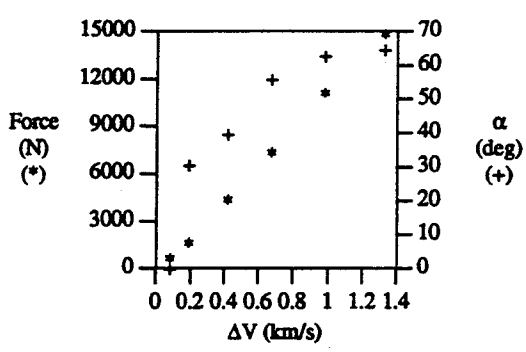

Fig. 8. Minimum force results with no altitude constraint (Mars).

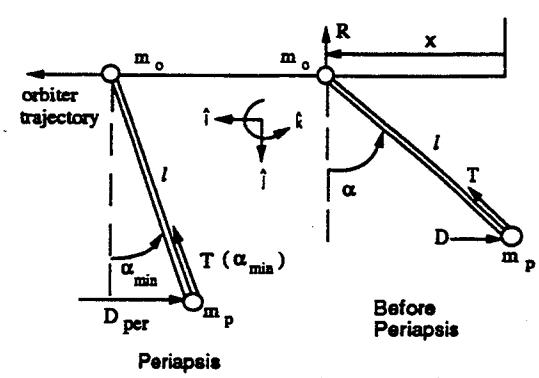

Fig. 9. Sliding pendulum.

which turns out to be about 95 s for Mars aerocapture. (Note that this value is very close to the actual fly-through times observed in the simulations in Figs 3–7.)

We can now derive the equations of motion for the sliding pendulum depicted in Fig. 9. Here we assume that the drag force, D, acts only on the probe. The orbiter is assumed to slide along a "frictionless wire" which provides a vertical reaction force, R. In this sliding pendulum there is no gravity. (The wire is, of course, a fictitious device which represents the horizontal trajectory of the orbiter). There are two degrees of freedom represented by the variables x and α; the unit vectors $\hat{\mathbf{i}}, \hat{\mathbf{j}}, \hat{\mathbf{k}}$ are fixed in the inertial reference frame.

The location of the center of mass of the tether system is given by

$$\mathbf{r} = (x - l_o \sin\alpha)\hat{\mathbf{i}} + l_o \cos\alpha\hat{\mathbf{j}} \tag{21}$$

where l_o is the distance from the orbiter to the center of mass:

$$l_o = \frac{l(m_p + \frac{1}{2}m_t)}{m} \tag{22}$$

and where m is the total mass,

$$m = m_o + m_t + m_p \tag{23}$$

Differentiating eqn (21) twice, we obtain

$$\ddot{\mathbf{r}} = (\ddot{x} - l_o\ddot{\alpha}\cos\alpha + l_o\dot{\alpha}^2\sin\alpha)\hat{\mathbf{i}} - (l_o\ddot{\alpha}\sin\alpha + l_o\dot{\alpha}^2\cos\alpha)\hat{\mathbf{j}} \tag{24}$$

Thus, from Newton's second law we have

$$\ddot{x} - l_o\ddot{\alpha}\cos\alpha + l_o\dot{\alpha}^2\sin\alpha = -\frac{D}{m} \tag{25}$$

$$l_o\ddot{\alpha}\sin\alpha + l_o\dot{\alpha}^2\cos\alpha = \frac{R}{m} \tag{26}$$

To remove the unknown, R, from eqn (26) we can use Euler's law

$$\mathbf{M}^c = \dot{\mathbf{H}}^c \tag{27}$$

The system angular momentum about the center of mass is

$$\mathbf{H}^c = I\dot{\alpha}\hat{\mathbf{k}} \tag{28}$$

where I is given by [15]:

$$I = m_o l_o^2 + \frac{m_t(l_o^3 + l_p^3)}{3l} + m_p l_p^2 \tag{29}$$

and where

$$l_p = \frac{l(m_o + \frac{1}{2}m_t)}{m}$$

$$l = l_o + l_p \tag{30}$$

The moment about the center of mass is

$$\mathbf{M}^c = (l_p D\cos\alpha - l_o R\sin\alpha)\hat{\mathbf{k}} \tag{31}$$

Substituting eqn (31) and the derivative of eqn (28) into eqn (27) provides

$$I\ddot{\alpha} = l_p D\cos\alpha - l_o R\sin\alpha \tag{32}$$

Eliminating R from eqns (32) and (26) we obtain

$$\ddot{\alpha} = \frac{l_p D\cos\alpha - ml_o^2\dot{\alpha}^2\cos\alpha\sin\alpha}{I + ml_o^2\sin^2\alpha} \tag{33}$$

Equations (25) and (33) provide the final equations of motion. Our main goal in deriving these equations is to provide an expression for the tension in the tether. This is most easily obtained by considering Newton's law for the orbiter, which moves along the x direction and is subject to a single force component along x:

$$m_o\ddot{x} = -T\sin\alpha \tag{34}$$

Thus, the tension is

$$T = -\frac{m_o\ddot{x}}{\sin\alpha} \tag{35}$$

Substituting for $\ddot{x}$ from eqn (25) into eqn (35), we obtain

$$T = \frac{m_o D}{m\sin\alpha} - \frac{m_o l_o\ddot{\alpha}\cos\alpha}{\sin\alpha} + m_o l_o\dot{\alpha}^2 \tag{36}$$

Next, we can eliminate $\ddot{\alpha}$ in eqn (36) through expression (33) to obtain our final relation for the tension:

$$T = \frac{Dm_o}{m\sin\alpha}\left(1 - \frac{ml_o l_p\cos^2\alpha}{I + ml_o^2\sin^2\alpha}\right) + m_o l_o\dot{\alpha}^2\left(1 + \frac{ml_o^2\cos^2\alpha}{I + ml_o^2\sin^2\alpha}\right) \tag{37}$$

Our hypothesis is that the minimum force maneuver maintains a nearly constant tether tension during fly through, so that if we can calculate the value of T at two points in the atmosphere and set the two values equal, then we may find an approximate value for the optimal α_{min} (given in Table 2 for Mars).

The tension comes from two sources: spin tension and drag tension. Naturally, before the tether enters the atmosphere it is subjected to only spin tension, but upon entry, drag tension becomes apparent. Of course as the tether translates through the atmosphere the moment from the drag force reduces the spin rate and hence the spin tension. When the spin rate becomes zero

$$\dot{\alpha} = 0 \tag{38}$$

the system reaches its minimum orientation, α_{min}, and eqn (37) becomes

$$T(\alpha_{min}) = \frac{D_{per}m_o}{m\sin\alpha_{min}}\left(1 - \frac{ml_o l_p\cos^2\alpha_{min}}{I + ml_o^2\sin^2\alpha_{min}}\right) \tag{39}$$

At an earlier stage, as the tether just enters the sensible atmosphere, a suitable value for the entry α can be chosen, α_{entry}, where the spin rate $\dot{\alpha}_{entry}$ has not been significantly altered and where drag tension is an

important effect. Following the approach of [9] and [15], we can determine the change in spin rate from the law of angular impulse and angular momentum. We assume that the linear impulse, P, is applied at the probe to cause the required change in velocity, ΔV:

$$P = (m_o + m_t + m_p)\Delta V \tag{40}$$

At the time of closest approach, the orientation of the tether is tilted by an angle α_{min}. The angular impulse at this orientation is given by

$$Pl_p \cos \alpha_{min} = I\Delta\Omega \tag{41}$$

where the reference point is the center of mass, $\Delta\Omega$ is the change in inertial spin rate and $I\Delta\Omega$ is, of course, the change in angular momentum.

From eqns (41), (40) and (30) we find that the change in spin rate is

$$\Delta\Omega = \frac{(m_o + \frac{1}{2}m_t)l}{I} \Delta V \cos \alpha_{min} \tag{42}$$

Keeping in mind the spin matching condition (1) and that $\dot{\alpha}$ can be approximated by the inertial spin rate, Ω, we have

$$\dot{\alpha}_{entry} \approx \Omega_{in} = -\tfrac{1}{2}\Delta\Omega \tag{43}$$

At α_{entry} we can determine the tension from drag by using the exponential atmosphere relation

$$D_{entry} = D_{per} \exp[-l(\cos \alpha_{min} - \cos \alpha_{entry})/H] \tag{44}$$

so that the total tension is found by substituting eqns (43) and (44) into eqn (37). The only remaining issue is to estimate the value of α_{entry}. Heuristically, we find that

$$\alpha_{entry} \approx 90° \tag{45}$$

Intuitively, eqn (45) seems reasonable because at 90° no appreciable spin rate change can occur, and yet the effect of drag must be noticeable since at this point the probe is only one tether length above its lowest altitude in the atmosphere. For the tether designs given in Table 1, this altitude is only $1.8H$, which will provide some drag tension. Thus, our expression from eqn (37) becomes

$$T(\alpha_{entry}) = \frac{m_o}{m} D_{entry} + m_o l_o \left[\frac{(m_o + \frac{1}{2}m_t)l}{2I} \Delta V \cos \alpha_{min}\right]^2 \tag{46}$$

We can now equate relations (39) and (46) to solve for α_{min}:

$$f(\alpha_{min}) = T(\alpha_{entry}) - T(\alpha_{min}) = 0 \tag{47}$$

Table 2 shows the results of eqn (47) in parentheses. These are in surprisingly close agreement with the optimal force solutions.

3.3. Minimum mass analysis

In order to analyze the tether mass problem, the dimensions of the tether, diameter d and length l, must be included in the analysis. However, since we want the tether to be only strong enough to withstand the forces in a particular maneuver, we can eliminate the diameter from the optimization space. The minimization can then be defined as:

$$\text{minimize:} \quad m_t(x)$$

$$\mathbf{x} = [\alpha_0, \dot{\alpha}_0, r_{per}, l]^t \tag{48}$$

$$\text{subject to:} \quad e - e_c = 0 \tag{49}$$

$$\Delta h - \Delta h_c > 0 \tag{50}$$

$$T_{min} > 0 \tag{51}$$

where m_t is the tether mass. (Note that the computation of m_t, for a given vector $\mathbf{x}$, includes the numerical (iterative) determination of the tether diameter required by the forces due to that particular maneuver. This, along with the inclusion of the length as a fourth dimension in $\mathbf{x}$, increases the number of iterations, and increases the required CPU time significantly.)

Before proceeding to the numerical computation of optimal tether masses for the various solar system bodies, we first consider an analytic approach which may be able to predict the characteristics of the optimal mass solution. We have already seen in the minimum force analysis that the minimum force often occurs at non-zero α_{min}. This leads to the possibility that a minimum mass solution may exist at some non-zero α_{min}.

We also observe that another minimum mass candidate solution is the vertical dumbbell maneuver. This solution has the great advantage of being easy to calculate from eqn (7). Thus we have two candidate solutions for minimum mass: (i) the vertical dumbbell maneuver ($\alpha_{min} = 0$) and (ii) the inclined maneuver ($\alpha_{min} > 0$).

We can find an approximate analytic solution for the inclined maneuver by the following procedure. First we take the characteristics of the vertical dumbbell tether given in Table 1 ($\Delta V, m_t, l, T, H, V_{lc}, r_{per}, e$) where all the values are calculated analytically. [For example we find T from eqn (9), we estimate r_{per} to be several scale heights above the planetary radius, and we compute V_{lc} from $\sqrt{\mu/r_{per}}$.] We assume that the clearance altitude is given by $\Delta h_c = l_{design}$ (where l_{design} is the design length given in Table 1). Next we substitute these characteristic design values into eqn (47) and solve for α_{min}. Naturally the resulting value will be non-zero which means that the clearance requirement ($\Delta h > \Delta h_c$) will no longer be satisfied. Thus we must correct our estimate of the tether length, l, by the following expression

$$l = \Delta h_c / \cos(\alpha_{min}) \tag{52}$$

In the next step we substitute the new value of l into eqn (47) to find a new α_{min}. After a few iterations (which can be performed on a hand calculator) we converge to a solution which provides an α_{min} that satisfies the minimum force condition (47) and the

Table 3. Analytic prediction for optimal tether mass

	Vertical dumbbell solution ($\alpha_{min} = 0$)			Inclined solution ($\alpha_{min} > 0$)			
Body	m_t (kg)	T (N)	l (km)	m_t (kg)	T (N)	l (km)	α_{min} (degrees)
Venus	31.0	5670	10.8	26.9	4500	12.6	31.0
Earth	38.0	8450	9.0	32.8	6070	10.8	33.7
Mars	112.0	15500	14.5	67.4	6570	20.6	45.2
Jupiter	18.0	1010	36.1	28.5	1560	37.1	13.5
Saturn	42.0	1550	54.4	45.6	1790	57.9	20.0
Uranus	63.0	1720	72.7	72.9	1840	78.7	22.5
Neptune	29.0	795	72.7	40.8	1070	75.7	16.1
Titan	426.0	10100	84.2	298.0	5330	112.0	41.0

altitude clearance (52). However, this solution still assumes the original design mass m_{design} (from Table 1) which is no longer correct because the length and the strength requirement have changed. We can compute a new estimate of the tether mass from

$$m_t = (l/l_{design})[T(\alpha_{min})/T_{design}]m_{design} \qquad (53)$$

where "design" refers to the values in Table 1. Substituting the new estimate of m_t into eqn (47), and repeating the above procedure, we converge to new values for l and α_{min}. If the values change significantly, we can repeat the process with a more refined estimate of m_t from (53).

The results of the iterative procedure are presented in Table 3 under the heading "inclined solution", where we used the precise value for r_{per} in Table 1 (which was obtained from simulation). For convenient comparison we also present the analytical results from the vertical dumbbell solution. The predictions of Table 3 from the analytic approach are quite interesting. According to the table, the optimal mass maneuver for Venus, Earth, Mars and Titan is an inclined maneuver, while the vertical dumbbell maneuver is expected to be optimal for Jupiter, Saturn, Uranus and Neptune. In the cases of Venus, Saturn, Earth and Uranus the differences between the two candidate maneuvers are probably too small to be decisive, and await numerical optimization for the final judgement. On the other hand, the case of Jupiter clearly indicates a vertical dumbbell maneuver while the case of Mars clearly favors the inclined maneuver.

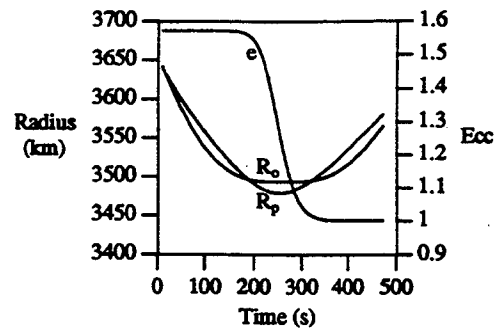

Fig. 11. End point positions and eccentricity (optimum mass trajectory).

Since the inclined case of Mars provokes some interest, we will first consider searching for its minimum mass by the numerical optimization techniques discussed earlier. In these computations we assume that $\Delta h_c = 14.5$ km and $e_c = 0.9999$. The resulting optimum tether system has a length of 20.7 km (an increase) and a diameter of 1.51 mm. These parameters represent a tether mass of only 66.4 kg, a saving of almost 41% over the tether system in Table 1 and 74% over propellant mass. We note that the close agreement of the optimal result with the analytic result presented in Table 3 is rather remarkable. In addition, the resulting inclined maneuver (Figs 10–12) presents some clear advantages over the vertical dumbbell maneuver. First, the spin rates before and after the maneuver are much smaller, eliminating the need for large fuel expenditures to generate spin rate. The fly-through attitude of about 45° maintains

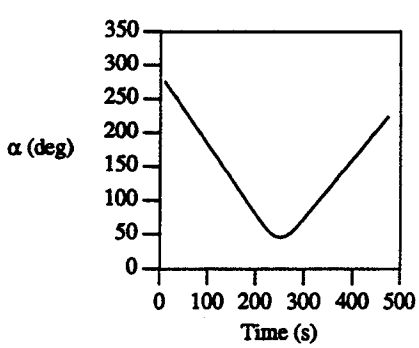

Fig. 10. Orientation angle (optimum mass trajectory).

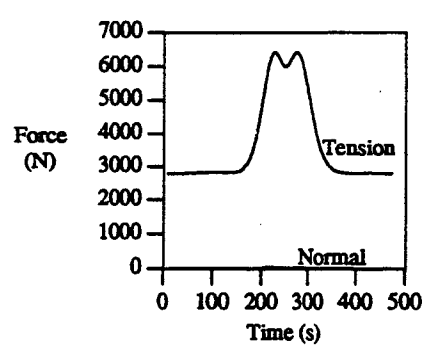

Fig. 12. Tether forces on the probe (optimum mass trajectory).

Table 4. Aerocapture results for solar system exploration (optimal mass)

Values	Venus	Earth	Mars	Jupiter	Saturn	Uranus	Neptune	Titan
ΔV(km/s)	0.35	0.39	0.67	0.27	0.41	0.50	0.34	1.31
Propellant mass (kg)	126	142	256	96	149	185	122	559
Tether mass (kg)	25.9	30.5	66.4	18.8	44.1	67.2	32.6	282
Savings (%)	79%	79%	74%	80%	70%	64%	73%	50%
Savings (kg)	99.1	112	190	77.2	105	118	89	277
Length (km)	12.4	10.5	20.7	36.1	54.4	72.7	72.8	112
Diameter (mm)	1.22	1.43	1.51	0.607	0.757	0.809	0.563	1.33
Probe area (m^2)	999	818	605	2370	1910	1810	2670	747
Maximum force (N)	4180	5820	6420	1050	1630	1850	899	5030
Minimum α (degrees)	27.7	28.4	45	0.46	0.18	0.27	0.75	41
Maneuver type†	I	I	I	V	V	V	V	I
Orbiter h_{min}(km)	145	103	95	495	848	1496	1246	540
Probe h_{min}(km)	135	94	80	459	794	1423	1173	456

†I = inclined, V = vertical.

significant (drag) tension on the tether throughout the maneuver (see Fig. 10) which should prevent it from bending despite the fact that the changes in tether dimensions create a system that (slightly) violates the center matching and aeromatching conditions. It is interesting to note that, even though it was never introduced as a requirement, spin matching is a feature of the optimum trajectory, as indicated by the equal tensions before and after fly through.

Table 4 presents the optimal mass for aerobraking tethers for solar system exploration. Again the orbiter and probe masses are assumed to be 1000 kg each, the tether is constructed of Hercules AS4 graphite and the capture orbit relative to the planet is assumed to have an eccentricity of 0.9999. [These are conditions (4)–(6) of the earlier tether design]. In addition we retain the probe areas of Table 1 and set Δh_c equal to the tether lengths in Table 1, which are given (to close approximation) by

$$\Delta h_c \approx 1.8H \tag{54}$$

The results of Table 4 show surprising agreement with the analytical predictions of Table 3. The analytical approach provides similar values for mass and length to the optimal solution and, furthermore, correctly determines whether the optimal maneuver is vertical or inclined.

One word of caution should be mentioned about checking the convergence of the numerical algorithm for the optimization problem. In all the available constrained optimization algorithms in the literature, the identification of the optimum solution is very important, from the points of view of stopping the iterative process and using the solution with confidence [13]. Generally speaking, one has two ways of checking for, at least, a local minimum. The first is by comparison with neighboring extremals (by perturbing the design vector near the candidate optimum, for example). Any such extremal should give a larger value of the final cost, or else, a lower value of the cost should be obtained only at the expense of violating one (or more) of the constraints. The second is by testing the Kuhn–Tucker conditions [14]. The first condition was checked for all the previous cases (the Kuhn–Tucker conditions were checked periodically) and were found to be satisfied (within a numerical error), providing at least a local minimum. The question of whether global minima can be found remains open at this stage. However, preliminary results presented in [20] provide a strong case that the minima given in Table 4 are, in fact, global.

4. CONCLUSIONS

The analytic approach presented here is remarkably accurate in predicting which of the two aerobraking strategies (vertical or inclined) will provide a lower tether mass. It is not yet known if the resulting solution is a global minimum. However, both maneuvers provide significant mass savings over propellant, suggesting a new option in the development of missions to the atmosphere-bearing planets.

Acknowledgements—The authors thank John Mechalas for assistance in computational work. This work has been supported in part by the National Science Foundation under Grant No. MSS-9114388.

REFERENCES

1. J. A. Carroll, Tether applications in space transportation. *Acta Astronautica* **13**, 165–174 (1986).
2. C. Purvis and P. Penzo, Multipass aerobraking of planetary probe. In *Tethers in Space Hand Book*, pp. 3.63–3.64. Office of Space Flight Advanced Programs (NASA), Washington, DC (1986).
3. S. W. Sirlin, R. A. Laskin, H. Otake and J. M. Longuski, Proposal to JPL director's discretionary fund FY '84: tethers for aerocapture and trajectory maneuvers. Jet Propulsion Laboratory, CA (1984).
4. E. C. Lorenzini, M. D. Grossi and M. Cosmo, Low altitude tethered Mars probe. *Acta Astronautica* **21**, 1–12 (1990).
5. T. W. Warnock and J. E. Cochran, Predicting the orbital lifetime of tethered satellite systems. *43rd IAF Congress*, Washington, DC (1992); *Acta Astronautica* **35**, 193–203 (1995).
6. J. Puig-Suari and J. M. Longuski, Modeling and analysis of tethers in an atmosphere. *Acta Astronautica* **25**, 679–686 (1991).
7. J. M. Longuski and J. Puig-Suari, Hyperbolic aerocapture and elliptic orbit transfer with tethers. *42nd IAF Congress*, Montreal, Canada (1991).

8. J. Puig-Suari and J. M. Longuski, Analysis of aerocapture with tethers. *AAS/AIAA Astrodynamics Conference*, AAS-91-549, Durango, CO (1991).
9. J. M. Longuski, J. Puig-Suari and J. Mechalas, Aerobraking tethers for the exploration of the solar system. *43rd IAF Congress*, Washington, DC (1992); *Acta Astronautica* **35**, 205–214 (1995).
10. J. Puig-Suari and J. M. Longuski, Aerocapture with a flexible tether. *AIAA/AAS Astrodynamics Conference*, AIAA-92-4662, Hilton Head Island, SC (1992).
11. J. Puig-Suari, J. M. Longuski and S. G. Tragesser, A three dimensional hinged-rod model for flexible-elastic aerobraking tethers. *AAS/AIAA Astrodynamics Conference*, AAS-93-730, Victoria, BC (1993).
12. C. T. Sun, Lectures on advanced composites. Class Notes for AAE 555, Composite Materials Laboratory, School of Aeronautics and Astronautics, Purdue University, West Lafayette, IN (1988).
13. S. S. Rao, *Optimization: Theory and Applications*. Wiley, New York (1984).
14. D. G. Luenberger, *Linear and Nonlinear Programming*, 2nd edition. Addison–Wesley, Reading, MA (1989).
15. J. Puig-Suari, Aerobraking tethers for the exploration of the solar system. Ph.D. thesis, School of Aeronautics and Astronautics, Purdue University, West Lafayette, IN (1993).
16. J. M. Longuski, Can aerogravity assist through the venusian atmosphere permit a near radial trajectory into the sun? Jet Propulsion Laboratory, Engineering Memorandum 312/82-133 (1982).
17. T. L. Vincent, Satellite life duration. *Am. Rocket Soc. Jl* **31**, 1015–1018 (1961).
18. N. X. Vinh, A. Busemann and R. D. Culp, *Hypersonic and Planetary Entry Flight Mechanics*. University of Michigan Press, Ann Arbor, MI (1980).
19. N. X. Vinh, *Optimal Trajectories in Atmospheric Flight*. Elsevier, New York (1981).
20. S. G. Tragesser, J. M. Longuski, J. Puig-Suari and J. P. Mechalas, Analysis of the optimal mass problem for aerobraking tethers. *AIAA/AAS Astrodynamics Conference*, AIAA-94-3747, Scottsdale, AZ (1994).